Breakdown of wind in turbulent thermal convection

Ronald du Puits, Christian Resagk, and André Thess
Ilmenau University of Technology, Department of Mechanical Engineering, P.O. Box 100565, 98684 Ilmenau, Germany
(Received 20 February 2006; revised manuscript received 22 June 2006; published 12 January 2007)

We report experiments on turbulent Rayleigh-Bénard convection of air in a cylindrical large-scale facility with a diameter of 7 meters and Rayleigh numbers up to $\mathrm{Ra}\approx 10^{12}$. The facility is used to explore the structure of the large-scale circulation for continuously varying aspect ratios between $\Gamma\approx 1$ and $\Gamma\approx 10$. Using autocorrelation functions derived from high-resolution time series of temperature and velocity near the cooling plate we demonstrate that the well-known single-roll structure (often called "wind") breaks down when the aspect ratio increases beyond the critical value $\Gamma_1=1.68\pm 0.22$. We further show that at $\Gamma_2=3.66\pm 0.46$ a second transition from an oscillatory two-roll structure to an unstable multi-roll structure takes place. The value of Γ_2 represents a lower bound for the aspect ratio that is necessary to reach homogeneous convection—a turbulent state that is free from the influence of lateral walls.

DOI: 10.1103/PhysRevE.75.016302 PACS number(s): 47.27.De, 05.65.+b

I. INTRODUCTION

Thermal convection in the atmosphere of the Earth and in stars is characterized by strong turbulence (implying very high Rayleigh numbers in the range $10^{12}\leqslant \mathrm{Ra}\leqslant 10^{21}$) and by a wide horizontal extent (exemplified by large aspect ratios $\Gamma>100$). Any attempt to investigate the structure of such flows in controlled laboratory experiments is complicated by the fact that it is currently impossible to simultaneously reach $\mathrm{Ra}>10^{13}$ and $\Gamma>100$. One can either obtain Rayleigh numbers up to $\mathrm{Ra}=10^{17}$ [1] in a narrow cylindrical cell by use of helium near the critical point ($\Gamma=0.5$) in which case the influence of lateral walls becomes dominant. Alternatively one can work with wide cells (e.g., $\Gamma=4$ [2] or $\Gamma=7.6$ [3,4]) up to $\mathrm{Ra}=10^{13}$ but it is impossible to vary the aspect ratio continuously. It is therefore of considerable interest to answer the following two questions: (1) What happens to the well-known large-scale circulation—the "wind" [5–7]—which is a characteristic feature of high Rayleigh number convection at $\Gamma\sim 1$ when the aspect ratio is gradually increased? (2) What is the value of the aspect ratio beyond which the influence of lateral walls becomes negligible and convection behaves effectively as laterally unbounded? Answering these questions requires convection experiments at high Rayleigh number and continuously adjustable aspect ratio—a requirement that no facility has satisfied up to now. The goal of the present paper is to describe a large-scale convection facility, the "Barrel of Ilmenau," and to report the first systematic exploration into the influence of the aspect ratio on the structure of the large-scale circulation in highly turbulent Rayleigh-Bénard convection.

Before describing the facility and our observations it should be emphasized that the existence of the wind in turbulent Rayleigh-Bénard convection at $\Gamma\sim 1$ and its coherent oscillation has been established more than a decade ago [5–7] on the basis of periodic fluctuations in local temperature signals. However, the origin of the oscillations remained unclear until Villermaux [8] proposed a first theoretical model for the observed periodicity in the temperature signals. He drew the picture that a plume from one plate is triggered by a plume from the opposite plate and all plumes organize themselves into a large single roll. This prediction was partially confirmed in helium experiments at Prandtl number $\mathrm{Pr}=0.7$ by correlation measurements between two temperature sensors [9,10] and later on also in water experiments $\mathrm{Pr}\approx 5$ by direct measurements of velocity [11–13]. However, recent results [14,15] indicate a more three-dimensional character of the convective flow in cubic as well as in cylindrical cells. Experimental and theoretical investigations by Resagk *et al.* [16] based on laser Doppler velocimetry (LDV) measurements near the boundary layer of the cooling plate and a dynamic model of Gledzer, Dolzhansky, and Obhukov [17,18] explain the influence of the geometry on the flow structure for the limited range $1<\Gamma<1.5$ but an experimental investigation for a wider range of Γ is still missing and occupies the rest of the present work.

II. EXPERIMENTAL SETUP

Our large-scale facility represents a classical Rayleigh-Bénard (RB) system. We use air in a cylindrical enclosure with a diameter $D=7.15$ m which is heated from below by an electrical heating system and cooled from above by a free-hanging water-cooled sandwiched aluminum plate with a weight of approximately 5 metric tons. An active compensation heating system prevents lateral heat losses and renders the sidewall effectively adiabatic. The temperature of the heating plate can be adjusted between 20 °C and 80 °C whereas the cooling plate is kept at 20 °C. Since the distance H between the heating and cooling plate is freely adjustable in the range $0.05\ \mathrm{m}<H<6.30\ \mathrm{m}$ we can continuously vary the aspect ratio of our system. A detailed description of the Barrel of Ilmenau will be given elsewhere [19].

The considered system is characterized by three dimensionless parameters, the Rayleigh number $\mathrm{Ra}=\alpha g\Delta T H^3/\nu\kappa$, the Prandtl number $\mathrm{Pr}=\nu/\kappa$, and the aspect ratio $\Gamma=D/H$. In these definitions α is the isobaric thermal expansion coefficient, g the acceleration of gravity, ΔT the temperature difference between both horizontal plates, ν the kinematic viscosity, and κ the thermal diffusivity. The Prandtl number in our experiment $\mathrm{Pr}=0.7$ is fixed by the thermophysical properties of air. In the experiments reported below we keep the

 ©2007 The American Physical Society

TABLE I. Summary of the properties of the temporal autocorrelation function of velocity (Φ_v, Φ_ϕ) and temperature signals (Φ_T) in all experiments. "+" denotes oscillation of $\Phi(\tau)$, "−" denotes absence of oscillation and "+−" stands for occasional oscillation with varying time scales, τ_v, τ_ϕ, and τ_T are the characteristic time scales of the oscillation.

Ra	Γ	Φ_v	τ_v [s]	Φ_ϕ	τ_ϕ [s]	Φ_T	τ_T [s]	τ_{LSC} [s]
7.48×10^{11}	1.13	−	−	+	43.4	−	−	53.6
3.47×10^{11}	1.47	−	−	+	38.5	−	−	40.8
1.62×10^{11}	1.89	+	103	−	−	+	109	−
7.42×10^{10}	2.45	+−	137	−	−	+	121	−
3.46×10^{10}	3.15	+	115	−	−	+	115	−
1.62×10^{10}	4.06	−	−	+	71	+	105	−
7.43×10^{9}	5.26	−	−	+	90	+−	−	−
3.37×10^{9}	6.81	−	−	−	−	+−	−	−
1.51×10^{9}	8.83	−	−	−	−	+−	−	−
7.16×10^{8}	11.3	−	−	−	−	+−	−	−

temperature difference $\Delta T=40$ K constant and study ten values of the aspect ratio starting from $\Gamma=1.13$ ($\mathrm{Ra}=7.48\times10^{11}$) to $\Gamma=11.3$ ($\mathrm{Ra}=7.16\times10^{8}$) [22]. The full parameter set of our experiments is summarized in Table I.

We perform local measurements of temperature and of the two horizontal velocity components along the central axis of the box in a distance up to 90 mm away from the cooling plate (see Fig. 1). A detailed description of the measurement techniques will be published in [19], hence we give only a brief account here. We arrange two single LDV probes with different orientation so that their measurement volumes coincide in the same point of space and provide time series for both components v_x and v_y. Both probes are mounted on a high-precision traverse system and can be moved in vertical (z) direction. Time series of v_x and v_y over one hour are captured at different z positions for all investigated aspect ratios. Here we are mainly interested in the velocity at a distance of $z=90$ mm ($z/H=0.025$) from the cooling plate which is outside the thermal boundary layer. By means of a linear interpolation algorithm the data for both velocity components are transformed into equidistant time series from which the magnitude $v=(v_x^2+v_y^2)^{1/2}$ and the angle $\phi=\arctan(v_y/v_x)$ are computed as functions of time. In order to analyze the temporal behavior of our flow in more detail we use the autocorrelation function (ACF) Φ which [for an arbitrary quantity $y(t)$] is defined as

$$\Phi_y(\tau)=\lim_{K\to\infty}\frac{1}{K}\sum_{i=1}^{K}y_i(t)y_i(t+\tau). \quad (1)$$

We typically use values between $K=5.000$ and $K=50.000$. Instead of the LDV probes a small microthermistor with size of approximately 100 μm can be mounted on the traverse system and time series of the temperature T are measured.

III. RESULTS

Let us start our discussion at the lowest aspect ratio $\Gamma=1.13$ for which $\mathrm{Ra}=7.5\times10^{11}$. Visual observation of the flow indicates the presence of a robust large-scale circulation consisting of a single roll, in agreement with earlier work. In the left column of Fig. 2(a) the ACF Φ_v, Φ_ϕ, and Φ_T are plotted. Whereas the fluctuations of v and T are clearly stochastic (i.e., $\Phi_v(\tau)\ll1$ and $\Phi_T(\tau)\ll1$), the ACF of $\phi(t)$ exhibits pronounced periodic oscillations. The time series of $\phi(t)$ shown in Fig. 3(a) confirms the oscillatory character of the turbulent flow. Two time scales can be extracted, namely, a shorter one with $\tau_\phi\approx43$ s and a second, significantly longer one with $\tau_\phi\approx500$ s. The short time scale corresponds to the cycle time $\tau_{LSC}=c/v_{\max}$ of the wind where c is the circumference of an ellipse with the half-axes $D/2$ and $H/2$ and $v_{\max}$ is the maximum magnitude of the velocity in the global flow measured at the central axis near the cooling plate. In fact the measured oscillation period slightly differs from τ_{LSC} for $\mathrm{Ra}=7.5\times10^{11}$ (cf. Table I), but the difference is probably due to the ambiguity in the estimation of the path length of the wind.

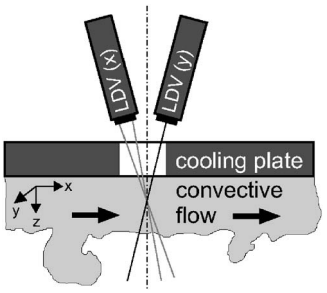

FIG. 1. Experimental setup: Two-dimensional LDV measurement of horizontal velocity in RB convection.

The interpretation of the second time scale is more subtle. It was recently proposed in [16] (building on earlier work by Dolzhansky [17]) that the oscillations of the large-scale circulation in turbulent Rayleigh-Bénard convection are mathematically similar to the dynamics of a heavy top, known from classical mechanics. In this rational framework the large time scale would be the fluid-dynamical counterpart to the precession of a heavy top and would depend on small departures of our geometry from perfect circular shape.

Our direct measurements of both horizontal velocity components confirm the visual observations of Funfschilling and Ahlers [15] who draw a picture of a single large convection roll with a rotation axis which oscillates periodically. In contrast to their experiments at $\mathrm{Pr}\approx5$ in our $\mathrm{Pr}=0.7$ experiment at $\Gamma\approx1$ neither axis rotations nor reversals of the wind could be observed. This is shown in the upper time series of Fig. 3 where the azimuthal angle of the velocity vector is plotted as a function of time. Clearly, $-100°<\phi<50°$ and no reversals are seen.

Upon increasing the aspect ratio to the next value $\Gamma=1.47$ ($\mathrm{Ra}=3.5\times10^{11}$) we observe that the properties of the flow remain virtually unchanged. Periodic oscillations in the azimuthal angle still exist, and $\phi(t)$ looks similar to Fig. 3(a). Surprisingly, however, the maximum of the horizontal velocity near the cooling plate grows despite the decreasing Rayleigh number. This is shown in Fig. 4 where we plot the maximum of the velocity scaled with the free-fall velocity $v_G=\sqrt{\alpha g\Delta TH}$ and the maximum of the velocity fluctuations.

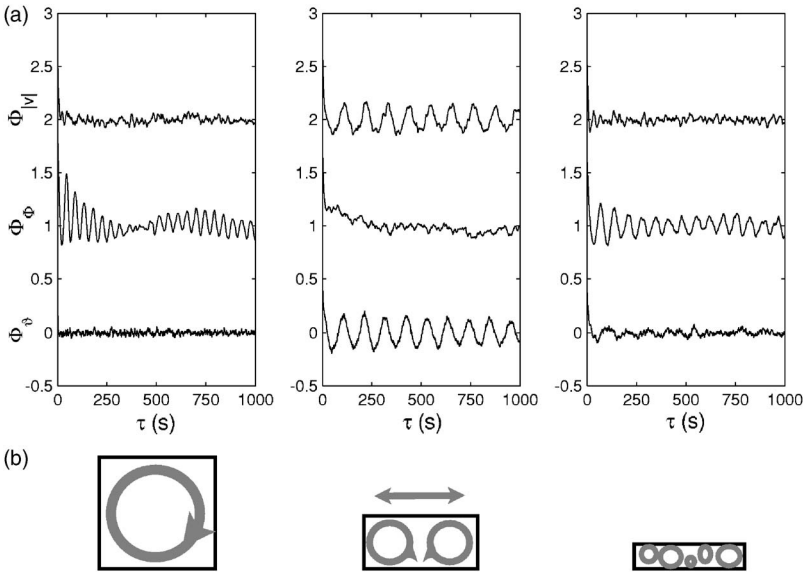

FIG. 2. Autocorrelation functions of the magnitude of velocity Φ_v (shifted by +2), angle of velocity relative to a fixed direction Φ_ϕ (shifted by +1) and temperature Φ_T for the three aspect ratios $\Gamma=1.13$ (left), $\Gamma=1.89$ (center), and $\Gamma=4.06$ (right) (a) together with sketches of hypothetic flow pattern that would match observations (b).

While the magnitude of the velocity grows the maximum of the velocity fluctuations and the angle covered by the oscillation of the large convective roll (not shown) decrease. The same effect was observed by Qiu and Tong [20] in a smaller water cell with $\Gamma=1.5$ but a convincing explanation is still lacking.

When we increase the aspect ratio to $\Gamma=1.89$, a dramatic change in the flow takes place. As shown in the middle column of Fig. 2, the ACF of the angle which previously showed pronounced oscillations becomes almost entirely structureless. Instead, the velocity magnitude and temperature exhibit oscillatory behavior. Taken into account the mass conservation argument the existence of periodic fluctuations in the magnitude of the horizontal velocity and the temperature immediately imply a recurrent vertical flow in the central axis of the experiment. As Fig. 3(b) also illustrates, $\phi(t)$ behaves erratic and displays occasional large excursions. Figure 4 shows that for $\Gamma \geqslant 1.89$ the normalized velocity $v_{\max}/v_G$ (and also $v_{\max}$, not shown) slightly decreases whereas $\sigma_{\max}$ grows. The observations from Figs. 2 and 3 complemented by preliminary flow visualizations in the vertical plane of the test cell at $\Gamma=2$ [21] lead us to the conclusion that the single-roll structure (the wind) has broken down and has been replaced by a flow structure sketched in the middle column of Fig. 2(b). The existence of two coexisting rolls variable in shape and position could explain the observed time scales between 105 and 121 s (Table I) which are significantly longer than the cycle time of each single roll. Presently a theoretical model explaining this relation is still missing.

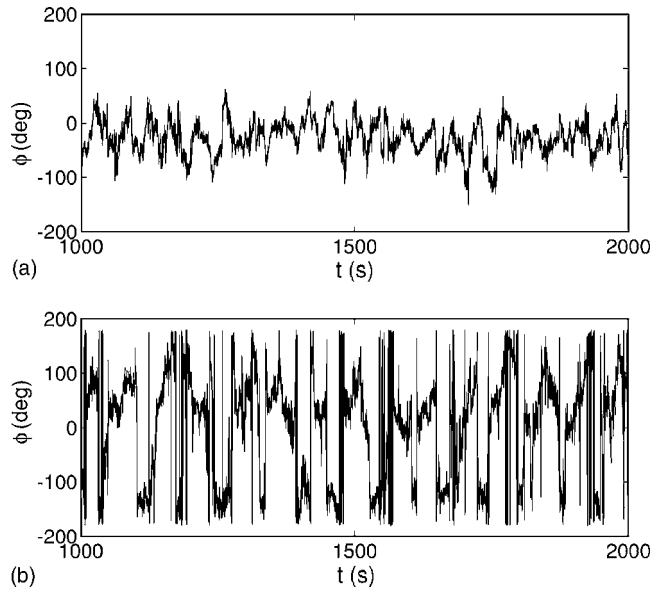

FIG. 3. Time series of the angle of the velocity vector measured in the center of the cylinder 90 mm below the cooling plate: $\Gamma=1.13$ (a) and $\Gamma=4.06$ (b).

When we increase the aspect ratio beyond a second threshold $\Gamma_2=3.66\pm0.46$, another transition takes place. Analyzing the standard deviation σ_ϕ of the angle $\phi(t)$, which is plotted in Fig. 5, a discontinuity between $\Gamma=3.15$ and $\Gamma=4.06$ can be clearly noted. While $\sigma_\phi < \pi/4$ for all aspect ratios $\Gamma \leqslant \Gamma_2$ this quantity jumps to $\sigma_\phi \approx \pi/2$ for $\Gamma \geqslant \Gamma_2$. This fact is reflected too in the time series of $\phi(t)$ [Fig. 3(b)] showing that the direction of the wind is permanently rotating although Fig. 2(a) (right column) provides evidence that the angle is still time correlated. In contrast, the velocity magnitude behaves randomly while the fluctuations of temperature are only occasionally time correlated. Eventually for

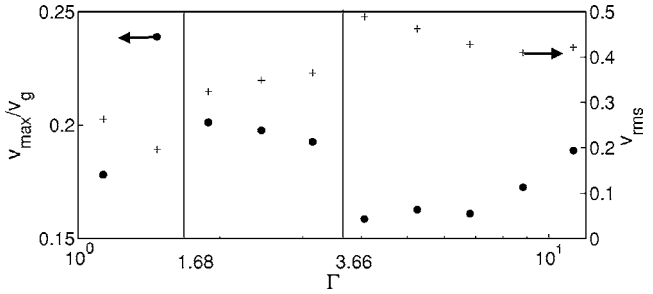

FIG. 4. Maximum of the horizontal velocity magnitude (circles) and its fluctuations (crosses) as a function of Γ. The velocity is normalized with the free-fall velocity v_g.

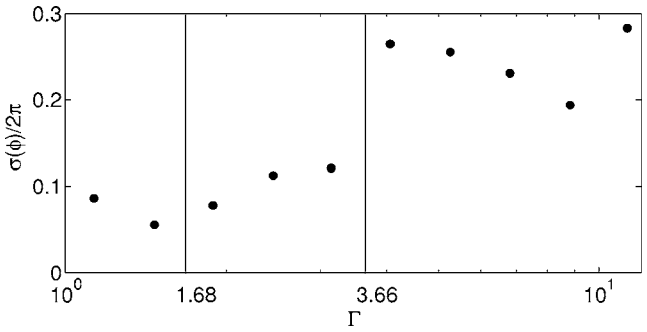

FIG. 5. Normalized standard deviation of the angle of the horizontal velocity vector as a function of Γ.

the highest $\Gamma=11.3$ the flow is completely uncorrelated. Table I summarizes the behavior for all aspect ratios. As far as our single-point local measurement allows, we can hypothesize that this final transition leads to a state with complex spatial structure, possibly consisting of multiple rolls. This finding is in a good agreement with the observation of Niemela and Sreenivasan [2] that the coherence of the wind is lost in a $\Gamma=4$ cell at $\mathrm{Ra}=6.5\times10^{11}$. Large-scale flow visualization and/or numerical simulations compared with these measurement results should bring even more light on the details of these phenomena and will be subject of our future work.

IV. CONCLUSION

In summary, we have demonstrated that the wind in turbulent Rayleigh-Bénard convection at high Rayleigh numbers ceases to exist once the aspect ratio of the cylindrical cell exceeds the critical value $\Gamma_1=1.68$. We suggest that beyond this value the flow is composed of two rolls undergoing coherent oscillations. Furthermore, we have shown that for even higher aspect ratios, namely, $\Gamma>\Gamma_2=3.66$, a second transition toward, a highly unstable regime takes place. However, it should be noted that this value is not necessarily universal and could be sensitive against Ra and Pr.

What has been gained with these results? Returning to the questions formulated in the Introduction, our determination of Γ_1 has certainly answered question (1) about the existence of the wind. By contrast, the identification of Γ_2 is at best a partial answer to the question (2) because Γ_2 is only a lower bound for the aspect ratio necessary to obtain turbulent convection that is free from the influence of side walls. Even if $\Gamma=3.66$ were the true threshold to "homogeneous" convection, experiments with $\mathrm{Ra}>10^{12}$ and $\Gamma>3.66$ would remain a challenge: To realize such a state we would have to build our barrel with a diameter of 23 meters!

ACKNOWLEDGMENTS

We thank Guenther Ahlers and Denis Funfschilling for very fruitful discussions and Vigimantas Mitschunas, Klaus Henschel, and Helmut Hoppe for invaluable technical help. Furthermore we wish to acknowledge both the Deutsche Forschungsgemeinschaft (Grants No. TH 497/16-1 and No. TH 497/16-2) as well as the Thueringer Ministerium fuer Wissenschaft, Forschung und Kunst for the financial support of the work reported here.

[1] J.-J. Niemela, L. Skrbek, K.-R. Sreenivasan, and R.-J. Donelly, Nature (London) **404**, 837 (2000).
[2] J.-J. Niemela and K.-R. Sreenivasan, J. Fluid Mech. **557**, 411 (2006).
[3] R.-L.-J. Fernandes and R.-J. Adrian, Exp. Therm. Fluid Sci. **26**, 355 (2002).
[4] R.-J. Adrian, R. T. D. S. Ferreira, and T. Boberg, Exp. Fluids **4**, 121 (1986).
[5] M. Sano, X.-Z. Wu, and A. Libchaber, Phys. Rev. A **40**, 6421 (1989).
[6] B. Castaing, G. Gunaratne, F. Heslot, L. Kadanoff, A. Libchaber, S. Thomae, X.-Z. Wu, S. Zaleski, and G.-M. Zanetti, J. Fluid Mech. **204**, 1 (1989).
[7] S. Ciliberto, S. Cioni, and C. Laroche, Phys. Rev. E **54**, R5901 (1996).
[8] E. Villermaux, Phys. Rev. Lett. **75**, 4618 (1995).
[9] J.-J. Niemela, L. Skrbek, K.-R. Sreenivasan, and R.-J. Donelly, J. Fluid Mech. **449**, 169 (2001).
[10] K.-R. Sreenivasan, A. Bershadskii, and J.-J. Niemela, Phys. Rev. E **65**, 056306 (2002).
[11] X.-L. Qiu and P. Tong, Phys. Rev. E **66**, 026308 (2002).
[12] K.-Q. Xia, C. Sun, and S.-Q. Zhou, Phys. Rev. E **68**, 066303 (2003).
[13] H.-D. Xi, S. Lam, and K.-Q. Xia, J. Fluid Mech. **503**, 47 (2004).
[14] T. Haramina and A. Tilgner, Phys. Rev. E **69**, 056306 (2004).
[15] D. Funfschilling and G. Ahlers, Phys. Rev. Lett. **92**, 194502 (2004).
[16] C. Resagk, R. du Puits, A. Thess, F. V. Dolzhansky, S. Grossmann, F. F. Arauio, and D. Lohse, Phys. Fluids **18**, 095105(2006).
[17] F. V. Dolzhansky, Izv. Akad. Nauk SSSR, Fiz. Atmos. Okeana **13**, 201 (1977) (in Russian).
[18] E. B. Gledzer, *Systems Of Hydrodynamic Type and Their Application* (in Russian) (Nauka, Moscow, 1982).
[19] R. du Puits, F.-H. Busse, C. Resagk, A. Tilgner, and A. Thess, J. Fluid Mech. **572**, 231(2007).
[20] X.-L. Qiu and P. Tong, Phys. Rev. E **64**, 036304 (2001).
[21] C. Resagk, R. du Puits, and A. Thess, Proceedings of 6th International Symposium on Flow Visualization, Pasadena, California, September 21–23, 2005.
[22] Variation of H, at $\Delta T=40$ K, in our experiment corresponds to moving along the curve $\mathrm{Ra}\,\Gamma^3=1.05\times10^{12}$.